J Shoulder Elbow Surg (2020) 29, e374–e385

ELSEVIER

Journal of Shoulder and Elbow Surgery

www.elsevier.com/locate/ymse

A new classification of impacted proximal humerus fractures based on the morpho-volumetric evaluation of humeral head bone loss with a 3D model

Raffaele Russo, MD[a,*], Antonio Guastafierro, MD[a], Giuseppe della Rotonda, MD[a], Stefano Viglione, MD[a], Michele Ciccarelli, MD[a], Marco Mortellaro, MSc[b], Paolo Minopoli, BSc[b], Fabrizio Fiorentino, BA[b], Livia Renata Pietroluongo, MSc[b]

[a]*Department of Orthopedic Surgery, Pineta Grande Hospital, Caserta, Italy*
[b]*E-lisa s.r.l., Naples, Italy*

Background: This study aimed to classify the pathomorphology of impacted proximal humeral fractures according to the control volume theory, with the intention to introduce a severity index to support surgeons in decision making.
Methods: In total, 50 proximal humeral fractures were randomly selected from 200 medical records of adult patients treated from 2009 to 2016. Four nonindependent observers used 2 different imaging modalities (computed tomography scans plus volume rendering; 3D model) to test the classification reliability. A fracture classification system was created according to the control volume theory to provide simple and understandable patterns that would help surgeons make quick assessments. The impacted fractures table was generated based on an evaluation of the calcar condition, determined by the impairment of a defined volumetric area under the cephalic cup and the humeral head malposition. In addition to the main fracture pattern, the comminution degree (low, medium, high), providing important information on fracture severity, could also be evaluated.
Results: From 3D imaging, the inter- and intraobserver reliability revealed a *k* value (95% confidence interval) of 0.55 (0.50-0.60) and 0.91 (0.79-1.00), respectively, for the pattern code, and 0.52 (0.43-0.76) and 0.91 (0.56-0.96), respectively, for the comminution degree.
Conclusions: The new classification provides a useful synoptic framework for identifying complex fracture patterns. It can provide the surgeon with useful information for fracture analysis and may represent a good starting point for an automated system.
Level of evidence: Basic Science Study; Development of Classification System

Keywords: Control volume; proximal humeral fractures; classification; shoulder; calcar; 3D; fracture severity; comminution

Ideally, a fracture classification should be relevant, reliable, reproducible, logical, useful, and not a form of abstract memory testing.[2,11,20,29] A comprehensive classification should help orthopedic surgeons to characterize a fracture, estimate the prognosis, and make optimal therapeutic decisions, allowing a uniform comparison of similar conditions.[2,4,11,20,29] Audigé et al[1] recognized classification categories as clinically relevant entities that surgeons

No institutional review board approval was required for this basic science study.

*Reprint requests: Raffaele Russo, MD, Department of Orthopedic Surgery, Pineta Grande Hospital, Caserta, Italy.
E-mail address: raff.russo55@gmail.com (R. Russo).

1058-2746/$ - see front matter
https://doi.org/10.1016/j.jse.2020.02.022

should be able to use for diagnosis with sufficient confidence to limit misclassification and associated treatment errors. Foruria et al[10] highlighted how the fracture model and the displacement of the fragments are important factors and predictors of the final result in the treatment of proximal humeral fractures (PHFs).

Assistance with image interpretation, which is the starting point of classification, can therefore provide considerable insight from an applicative clinical perspective. Recent advances in artificial intelligence, particularly in neural networks, have shown important results and offer promising applications in the medical imaging field.[7,9,19,22] Machine learning systems help to identify patterns and associations that may normally evade human eyes.[7] In this type of approach, it is important to set up an analytical preparatory study to determine a rational basis that predisposes the analyzer to identify some key characteristics in the image. This method should allow artificial intelligence to be more effective and commit the fewest possible errors.

Although there is extensive literature on PHF, the foundation remains insufficient for a complex mathematical model to be developed as a clinically useful tool for surgeons. In a recent study, Russo et al[28] presented the control volume (CV) theory that demonstrated the existence of a mathematical rationale in head displacements in the PHFs: the link between humeral head displacement and the loss of volume under the head.

We believe that this theory can provide a starting point for the creation of a complex mathematical model that can serve as a basis for intelligent systems to assist in image interpretation. Nevertheless, the transition from the CV theory to an automated system, that exploits the principles of the theory to identify fracture patterns precisely, is not so immediate. Therefore, we consider it necessary to create a classification that, on the one hand, may be the beginning of an automated system and, on the other hand, can provide the surgeon with useful information for fracture analysis.

The main aim of this study is to present a new classification system for proximal impacted humeral fractures based on the CV theory, organized according to a severity concept among the different fracture patterns. The second aim of the current study is to introduce an assessment of the comminution degree as additional information on the CV conditions and fracture severity. Both aims are functional to the future development of an automated system to assist the surgeon in both the image interpretation and the choice of the most appropriate treatment.

Theoretical background for classification design

A relevant aspect of CV theory is to have demonstrated the pathologic link between the partial or total modification of the area and the relative displacement of the humeral head. Furthermore, there are some critical and questionable points of this theoretical assumption that the scientific community should consider. First, the α and β planes, used conventionally as a spatial reference system to delimit the CV, could become a new common reference for locating the most significant fracture lines. Secondly, accurate topographic evaluation of CV loss that can serve to justify the displacement of the humeral head analytically is difficult to calculate without the help of specific researchers. Thirdly, the high variability of fracture morphology could lead to a similar head displacement with equivalent CV loss, but that is associated with different severity due to high comminution or different topographical involvement.

The requirement for this methodology started with the CV theory and continues with a classification system that enriches it with useful information for the surgeon that the CV theory cannot provide. By defining a comminution degree of a bony part, it is possible to evaluate the CV condition from another point of view. In their studies, Beardsley et al[3,4] related the bone comminution to the energy of the trauma and used it as a measurement of articular injury severity. Higher energy input led to a greater number of fragments that were also smaller. The energy absorbed by bone during loading is released when the bone breaks; therefore, the more energy the bone can absorb and the greater the release in the event of a fracture, the greater the comminution will be.

The loading rate, patient age, and bone quality all affect the bone energy-absorption capacity.[6,8,23] The ductility of bones, as well as their ability to absorb energy before fracturing, shows an age-related decrease of approximately 5%-10% per decade. Moreover, bone that undergoes rapid loading will absorb more energy than when loaded at a slow rate. This phenomenon helps to explain why injuries with rapid loading and higher velocities dissipate greater energy and result in greater fracture comminution and displacement. Comminution is very important even when referred to the calcar; indeed, calcar comminution significantly decreases the stability of fracture reconstruction,[24] so its integrity is recognized in recent studies as a key factor, both in biomechanical and biological terms, for the success of fracture reconstruction interventions.[5,12,14-16,18,24]

Materials and methods

The study used a standardized protocol to retrospectively include the computed tomography (CT) scans of 200 consecutive acute PHFs in adults treated surgically from 2009 to 2016 by a senior surgeon (R.R.). The exclusion criteria were patients aged less than 18 years, with pathologic fractures, isolated tuberosity fractures, dislocations fractures, nonarticular fractures, and those with non-impacted fractures.

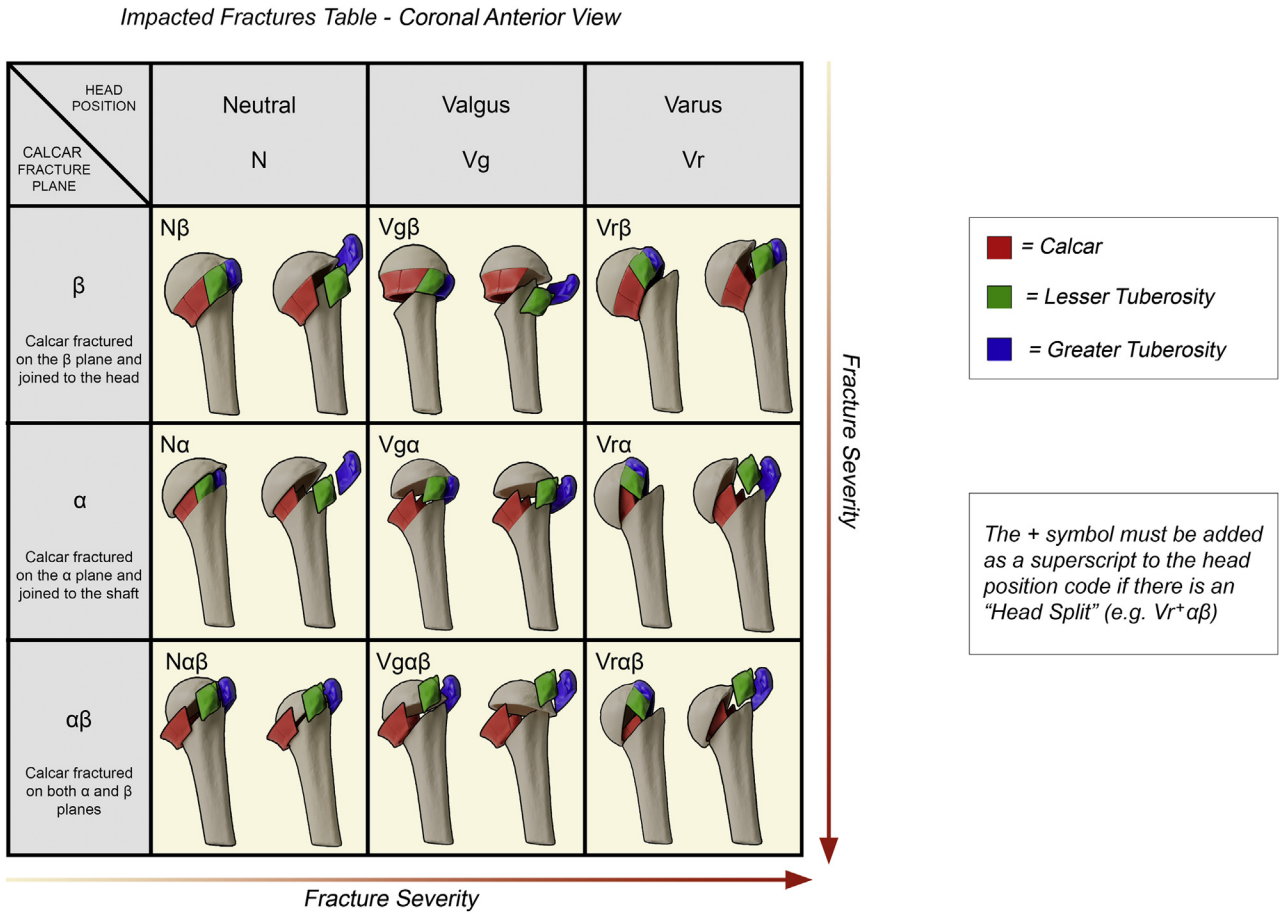

Figure 1 Impacted fractures table. The color legend of the control volume parts is shown to the right of the table. The red arrows indicate the increasing direction of the fracture pattern severity. Each fracture pattern is represented with 2 schematic analogic models displayed on the coronal plane. An example of the fracture code is shown in the lower-right box; the superscript "+" must be entered only if the head is split.

Table I Row criterion: the impairment of the α and β planes in relation to the calcar

β	This row includes all the fractures in which it is possible to identify the calcar fractured on the β plane and joined to the head (a minimum calcar of 8 mm in length must be recognizable)
α	This row includes all the fractures in which it is possible to identify the calcar fractured on the α plane and joined to the shaft
αβ	This row includes all the fractures in which it is possible to identify the calcar fractured on both α and β planes

From these 200 records, 50 were selected by simple randomization to test the reliability of the new classification system, using different imaging modalities. CT images were obtained using a 64-slice Somatom Sensation 64 CT scanner (Siemens, Erlangen, Germany) with a slice thickness of 0.6 mm. Axial, oblique coronal, and oblique sagittal images adapted to the plane of the shoulder were generated, and 3D volume rendering (VR) and 3D model reconstructions were obtained for all patients.

Impacted fractures table

Malposition of the humeral head and the calcar conditions, defined by the impairment of the α and β planes, were used to generate the impacted fractures table (Fig. 1). It was decided to represent each fracture pattern with 2 schematic analogic models displayed on the coronal plane.

The column criterion was head positions (malpositions) on the coronal plane, with reference to the positions defined by the CV theory:[28]

- neutral
- valgus
- varus.

The study of the CV provided important and precise aspects on how the humeral head could impact the underlying trabecular structures. This study clarified that the head, in addition to moving in the varus or valgus position, could also remain in a neutral position, findings that were likely to influence some therapeutic decisions.

The Row criterion is shown in Table I.

The cross between the 2 criteria generated an identification code for fracture patterns, as described in Table II.

Table II Description of the fracture patterns generated by the cross between the column and row criterion

Nβ	Vgβ	Vrβ
The head in neutral position and the calcar fractured on the β plane (separated from the shaft) and joined to the head	The head in valgus position and the calcar fractured on the β plane (separated from the shaft) but joined to the head	The head in varus position and the calcar fractured on the β plane (separated from the shaft) but joined to the head
Nα	**Vgα**	**Vrα**
The head in neutral position and the calcar fractured on the α plane (separated from the head) but joined to the shaft	The head in valgus position and the calcar fractured on the α plane (separated from the head) but joined to the shaft	The head in varus position and the calcar fractured on the α plane (separated from the head) but joined to the shaft
Nαβ	**Vgαβ**	**Vrαβ**
The head in neutral position and the calcar fractured on both α and β planes (separated both from the head and shaft) or the calcar no longer recognizable	The head in valgus position and the calcar fractured on both α and β planes (separated both from the head and shaft) or the calcar no longer recognizable	The head in varus position and the calcar fractured on both α and β planes (separated both from the head and shaft) or the calcar no longer recognizable

Table III Level of comminution for each part of the control volume

Level 0	0 fragments (not comminuted): whole part or fractured part but without fragments
Level 1	1 fragment: fractured part with a single fragment separated from the humerus. The fragment may be the part itself or a portion thereof
Level 2	2 fragments: fractured part with 2 fragments separated from the humerus. The fragments may be the part itself or a portion thereof
Level 3	3 or more fragments: fractured part in 3 or more fragments or nonmeasurable fragments

The code of the ''impacted fractures table'' could be completed, if required, with the addition of the superscript ''+'' symbol to indicate the presence of the head split that completed the pathomorphologic analysis of the fracture.

The input variables of the table were sorted according to a criterion of increasing severity from left to right for the rows, and from top to bottom for the columns (red arrows in Fig. 1). The severity concept can be linked to 3 different aspects as follows: fracture complexity in anatomic-pathologic terms (anatomic-pathologic severity), risk of humeral head necrosis (biological severity), and surgical reconstruction difficulty (mechanical severity). In the columns, a varus fracture is more severe than a fracture with the head in a neutral or valgus position because it may present a higher risk of humeral head necrosis. The choice of classification iconography is only based on humeral head displacements on the coronal plane, without considering those on the sagittal plane. This is due to the greater importance of varus or valgus displacement in the characterization of the fracture pattern, and in its severity concept: a varus displacement increases the risk of mechanical unbalance of cuff strength, humeral head ischemia, and the instability and necrosis of fragments. An impacted humeral head in valgus presupposes a subversion of the proximal humeral epiphysis anatomy according to the pathologic morphology of the great tuberosity modification with possible cuff involvement. In the literature, varus and valgus displacements are considered fundamental to fracture characterization,[27,30] in particular in the choice of treatment to be used to reposition the humeral head in the correct anatomic and biomechanical position.

Comminution table

In addition to the main fracture pattern, it is possible to evaluate a CV comminution degree (low, medium, high) to provide additional information and make the classification itself more complete. The comminution constitutes direct information on the technical demand of fracture repair[4] (the same fracture pattern presents more difficulties in reconstruction if it has a greater comminution degree) and indirect information on the energy of the trauma and the patient's bone quality.[3,4,6] The assessment of CV comminution (low, medium, high) provides important information on fracture damage (only from the bone standpoint and not vascularization or other) that could prove to be an excellent supplement to the main fracture pattern.

This additional indication was determined starting from the comminution level of the CV parts (calcar in the medial zone; lesser and greater tuberosities in the lateral zone). The comminution levels of a single part are shown in Table III.

A first evaluation must be made on the medial zone (calcar) where the comminution has a greater weight in the total bone loss of the CV. The comminution of the lateral zone, determined by the sum of the comminution level of the lesser tuberosity (Lt) and greater tuberosity (Gt), will complete the analysis and provide the

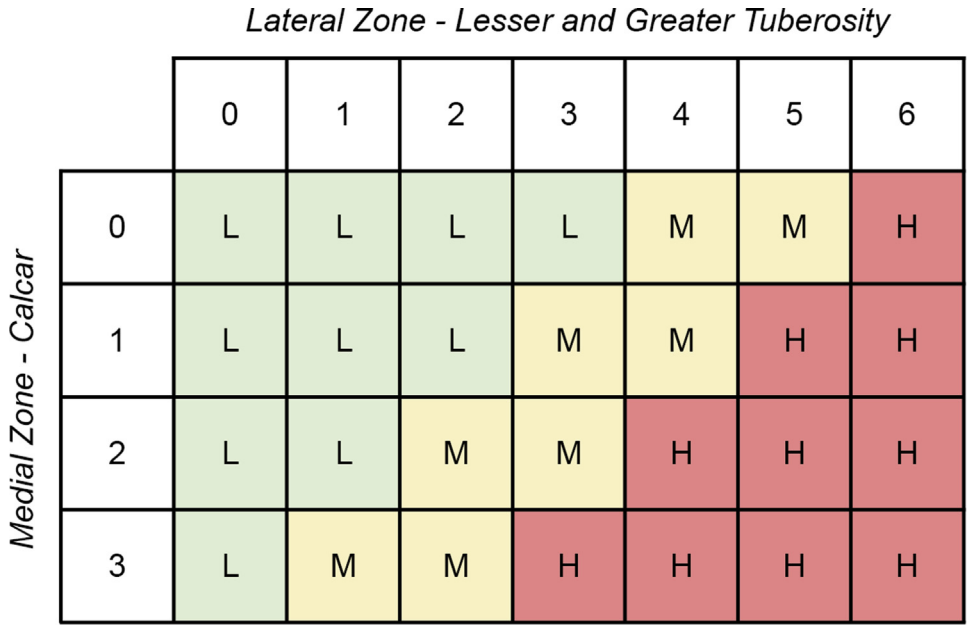

Figure 2 The comminution table. The rows refer to the level of comminution of the calcar (medial area), and the columns refer to the sum of the tuberosity comminution levels (lateral area). The cross between the comminution level of the medial and lateral zones provides the comminution grade of the control volume: L = low comminution, M = medium comminution, and H = high comminution.

Table IV Results of interobserver analysis

	Interobserver reliability							
	CT+VR				3D			
	k	Landis and Koch	95% CI	POA (%)	*k*	Landis and Koch	95% CI	POA (%)
Pattern code	0.41	Moderate	0.36-0.45	47	0.55	Moderate	0.5-0.6	60
Head position	0.49	Moderate	0.4-0.57	66	0.61	Substantial	0.52-0.69	74
Fracture planes	0.51	Moderate	0.42-0.6	67	0.63	Substantial	0.54-0.71	75
Head split	0.7	Substantial	0.59-0.81	85	0.82	Almost perfect	0.71-0.93	91
CV comminution	0.49	Moderate	0.4-0.57	66	0.52	Moderate	0.43-0.6	68

CV, control volume; *CT*, computed tomography; *VR*, volume rendering; *CI*, confidence interval; *POA*, percent of agreement.
The agreement was evaluated on the pattern code (18 options: 3 for head position, 3 for fracture plane, and 2 for head split) and on the comminution grade of control volume (3 options).

final value (low, medium, high) (Fig. 2) that is to be associated with the main fracture pattern.

Interobserver and intraobserver analysis

In total, 50 fractures were selected by simple randomization to test the reliability of the new classification system, using CT images and VR and a 3D model. The observed fractures concerned 30 women and 20 men, with 33 right shoulders and 17 left. The average age was 62 years (minimum, 18 years; maximum, 90 years). Four orthopedic surgeons from a single department (R.R., A.G., S.V., G.D.R.) were asked to classify the 50 fractures using the new classification system.

The examiners evaluated the 50 fractures twice independently and were not permitted to compare results. In the first evaluation, the examiners only had access to the tomographic images and the VR of the patients; in the second evaluation, they had only the 3D model of the fractures available. The 3D model was obtained with the aid of engineers who processed the tomography data through the software Mimics (Materialize, Belgium). It is worth noting that the 3D model allows the fragments to be moved, unlike the VR that generates a 3D view of the fracture but does not allow interaction with it. The 50 fractures were presented to the examiners at each evaluation in a different order (simple randomization) and anonymized to avoid patient memorization. All examiners knew the CV theory, and by comparing the examiners' evaluations, the interobserver reliability of the new classification system was determined. The intraobserver reliability was obtained by 1 observer (R.R.) who repeated the evaluation on the 50 fractures after a 4-month interval with the order of the anonymized fractures randomly switched.

Table V Results of intraobserver analysis (4 months)

	Intraobserver reliability							
	CT + VR				3D			
	k	Landis and Koch	95% CI	POA (%)	*k*	Landis and Koch	95% CI	POA (%)
Pattern code	0.57	Moderate	0.45-0.70	62	0.91	Moderate	0.79-1.00	92
Head position	0.61	Moderate	0.41-0.81	74	0.94	Substantial	0.74-1.00	96
Fracture planes	0.73	Moderate	0.51-0.95	82	0.94	Substantial	0.73-1.00	96
Head split	0.76	Substantial	0.48-1.00	88	1	Almost perfect	0.72-1.00	100
CV comminution	0.7	Moderate	0.50-0.90	80	0.76	Moderate	0.56-0.96	84

CV, control volume; *CT*, computed tomography; *VR*, volume rendering; *CI*, confidence interval; *POA*, percent of agreement.
The agreement was evaluated on the pattern code (18 options: 3 for head position, 3 for fracture plane, and 2 for head split) and on the comminution grade of control volume (3 options).

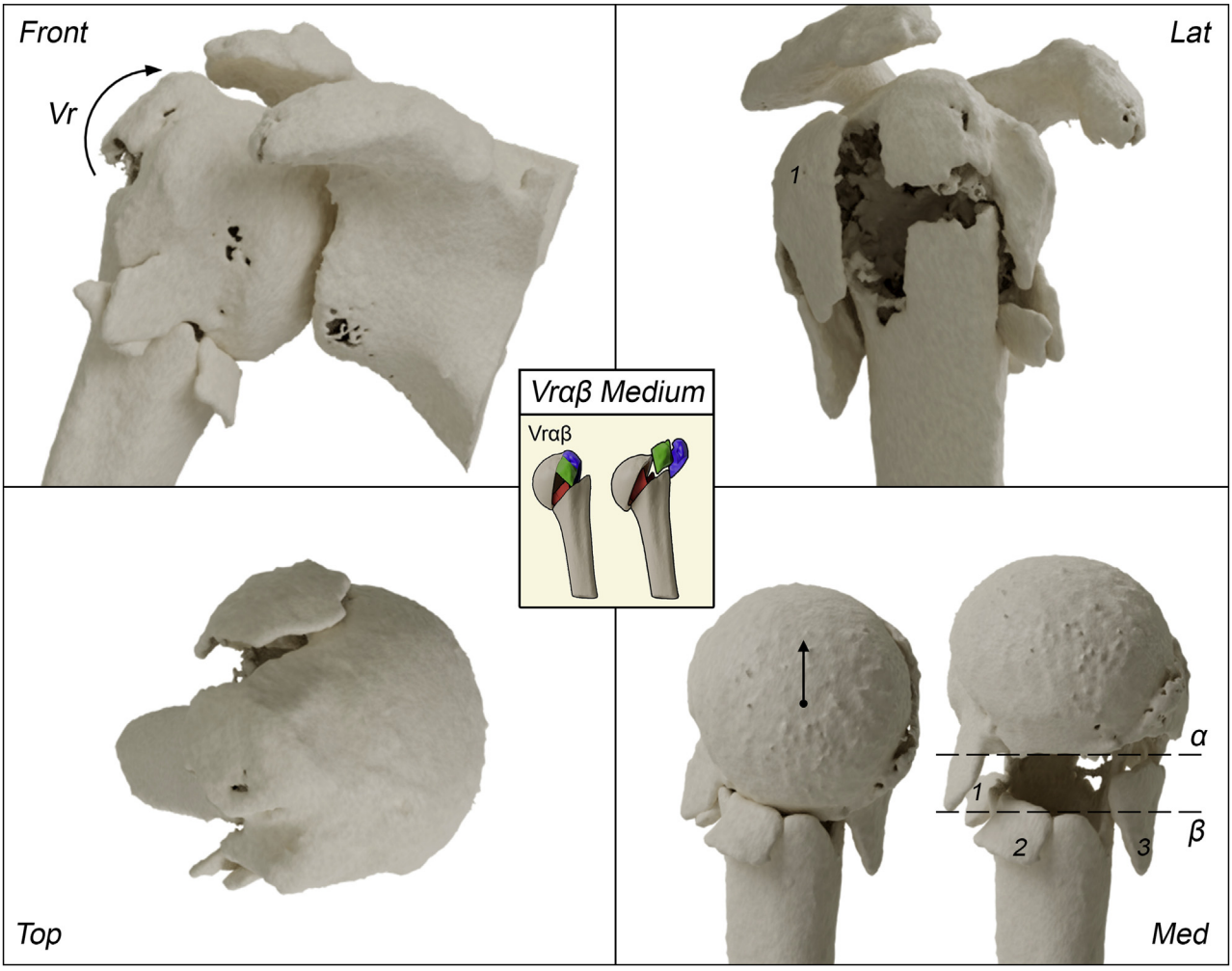

Figure 3 Example of a Vrαβ Medium fracture. 3D reconstruction of one of the 50 fractures analyzed. The 4 quarters show different views: Front (frontal), Lat (lateral), Top, and Med (medial). The corresponding fracture pattern is found in the center. In the frontal view, the curved arrow indicates the pathologic head displacement in varus (Vr). In the medial view, the arrow indicates the movement needed to the anatomic reposition of the head to better analyze the calcar conditions; the dashed line shows the calcar fracture lines on the α and β planes. Level 3 of the medial comminution and level 1 of the lateral comminution determine a ''medium comminution'' grade.

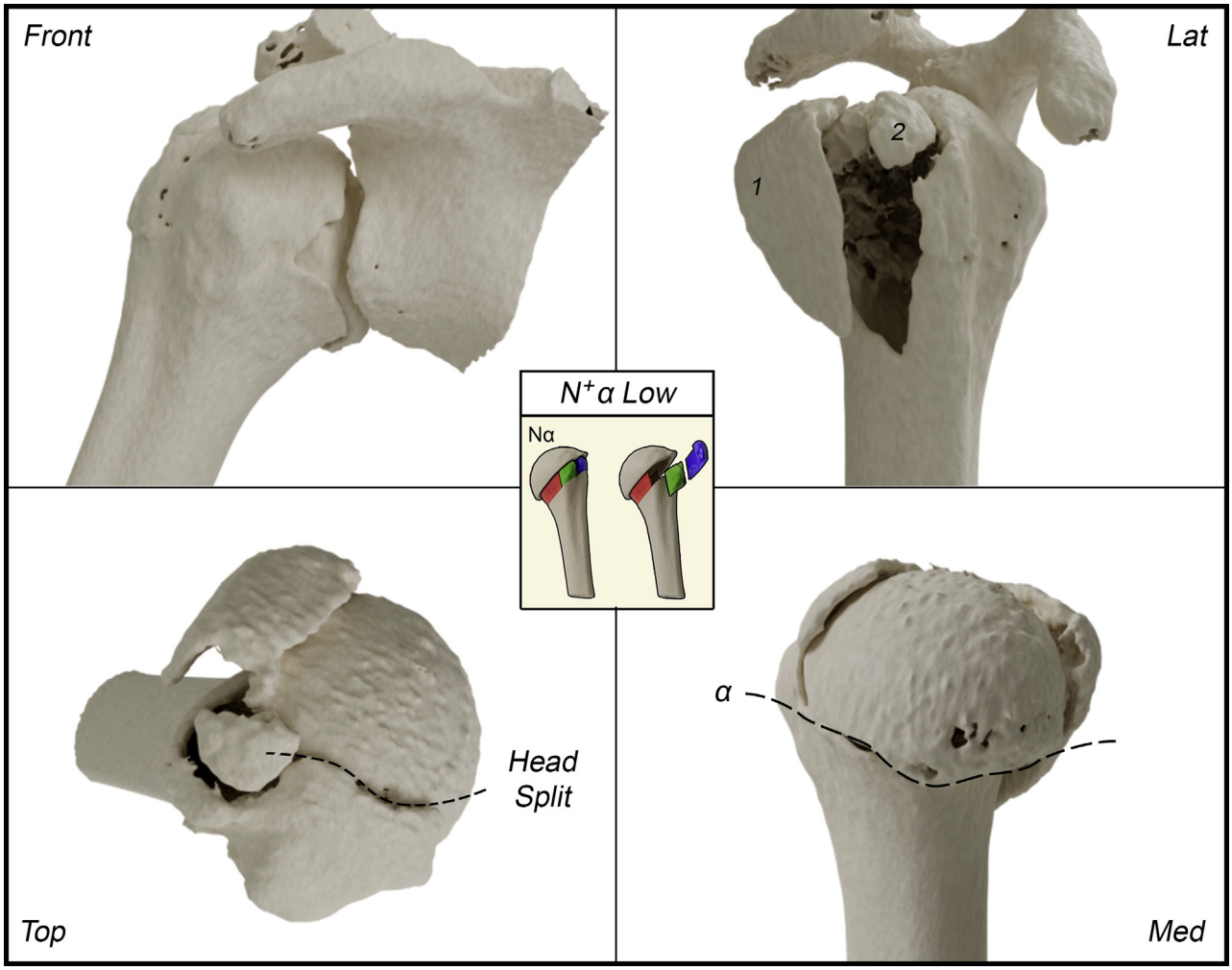

Figure 4 Example of a $N^{+}\alpha$ Low fracture. 3D reconstruction of one of the 50 fractures analyzed. The 4 quarters show different views: Front (frontal), Lat (lateral), Top, and Med (medial). The corresponding fracture pattern is shown in the center. In the frontal view, the neutral displacement of the head (N) is shown. In the top view, the dashed line highlights the head split (+). In the medial view, the dashed line shows the calcar fracture line on the α plane. The calcar is not comminuted (level 0), and there are only 2 fragments of the greater tuberosity (level 2 of lateral comminution); the comminution grade is ''low.''

Statistical analysis

Randolph's *k* statistical parameter, namely free-marginal multirater kappa,[26,32] with a 95% confidence interval was used for the evaluation of interobserver and intraobserver reliability. Randolph's *k* is recommended as an alternative to Fleiss' multirater kappa when the raters do not know a priori how cases are to be distributed in categories. The parameter *k* can take values from 1 to −1. Values between 1 and 0 indicate agreement better than chance, a value of 0 indicates a level of agreement that could have been expected by chance, and values between 0 and −1 indicate levels of agreement that are worse than chance. According to Landis and Koch,[17] the following intervals of *k* were considered: 0.00-0.20, slight agreement; 0.21-0.40, fair; 0.41-0.60, moderate; 0.61-0.80, substantial; and 0.81-1.00, almost perfect. The percentage of the proportion of overall agreement (POA) was also observed. All calculations were performed with the aid of electronic spreadsheets with Microsoft Excel software.

Results

The ''impacted fractures table'' and the ''comminution table'' (Figs 1 and 2) demonstrate the main results of this study. The results of inter- and intraobserver reliability are shown respectively in Tables IV and V.

The evaluation of the agreement on the pattern code of the ''impacted fractures table'' and on the CV comminution was reported. In the interobserver analysis, the pattern code had a moderate agreement with both the CT + VR imaging modality ($k = 0.41$; POA = 47%) and the 3D imaging modality ($k = 0.55$; POA = 60%). The CV comminution had a moderate agreement with both imaging modalities (CT + VR: $k = 0.49$; 3D: $k = 0.52$), but with a higher POA than the pattern code (CT + VR: POA = 66%; 3D: POA = 68%).

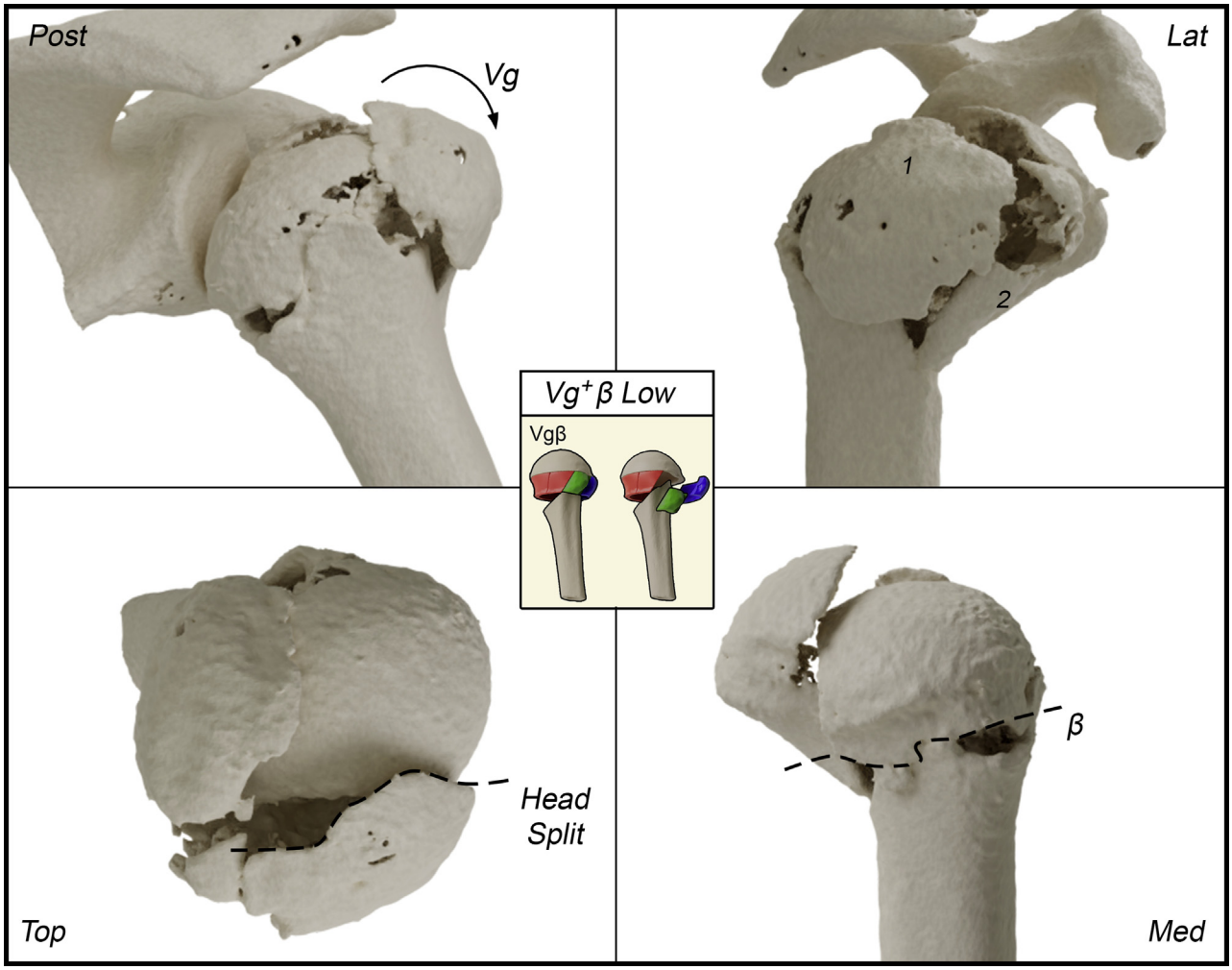

Figure 5 Example of a $Vg^{+}\beta$ Low fracture. 3D reconstruction of one of the 50 fractures analyzed. The 4 quarters show different views: Front (frontal), Lat (lateral), Top, and Med (medial). The corresponding fracture pattern is shown in the center. In the frontal view, the curved arrow indicates the pathologic head displacement in valgus (Vg). The calcar is fractured on the β plane but not comminuted (level 0), and the lateral area is only fractured in 2 fragments (greater tuberosity) determining a ''low comminution'' grade.

The agreement values on the head position, fracture planes, and head split showed the influence of these criteria on the pattern code agreement.

The head position had the least agreement ($k = 0.49$) despite a POA of 66%. This increased to substantial with the 3D imaging modality ($k = 0.61$; POA = 74%), probably because the 3D enables better visualization of the articular relationship between the head and glenoid, and therefore also of the movements between the head and shaft. The same trend can also be seen for the fracture planes, with slightly higher agreement values (CT + VR: $k = 0.51$; 3D: $k = 0.63$).

The head split had the highest agreement (CT + VR: $k = 0.70$; 3D: $k = 0.82$), both because it is a dichotomous variable and because it is easier to locate and assess the presence of damage to the humeral head with the aid of the VR and 3D model.

It is worth noting that the 3D imaging modality provided a greater agreement than the use of CT and VR in all cases. The interobserver agreement after 4 months was *almost perfect* and *substantial* with the 3D imaging modality.

Discussion

New innovative technologies to support orthopedic medicine are becoming valuable aids to improve and facilitate the performance of physicians, making them more precise, safer, and with better patient outcomes. Computer-assisted surgeries, augmented reality, 3D printing, artificial intelligence systems for diagnostic imaging, and many other futuristic applications are becoming more current.[7,13,25,31] Our study favors and respects this tendency toward technological innovation as it is aimed at creating an automated system to assist the surgeon in both image interpretation and the choice of the most appropriate treatment. As mentioned above, the transition from the CV theory to an automated system, which exploits the

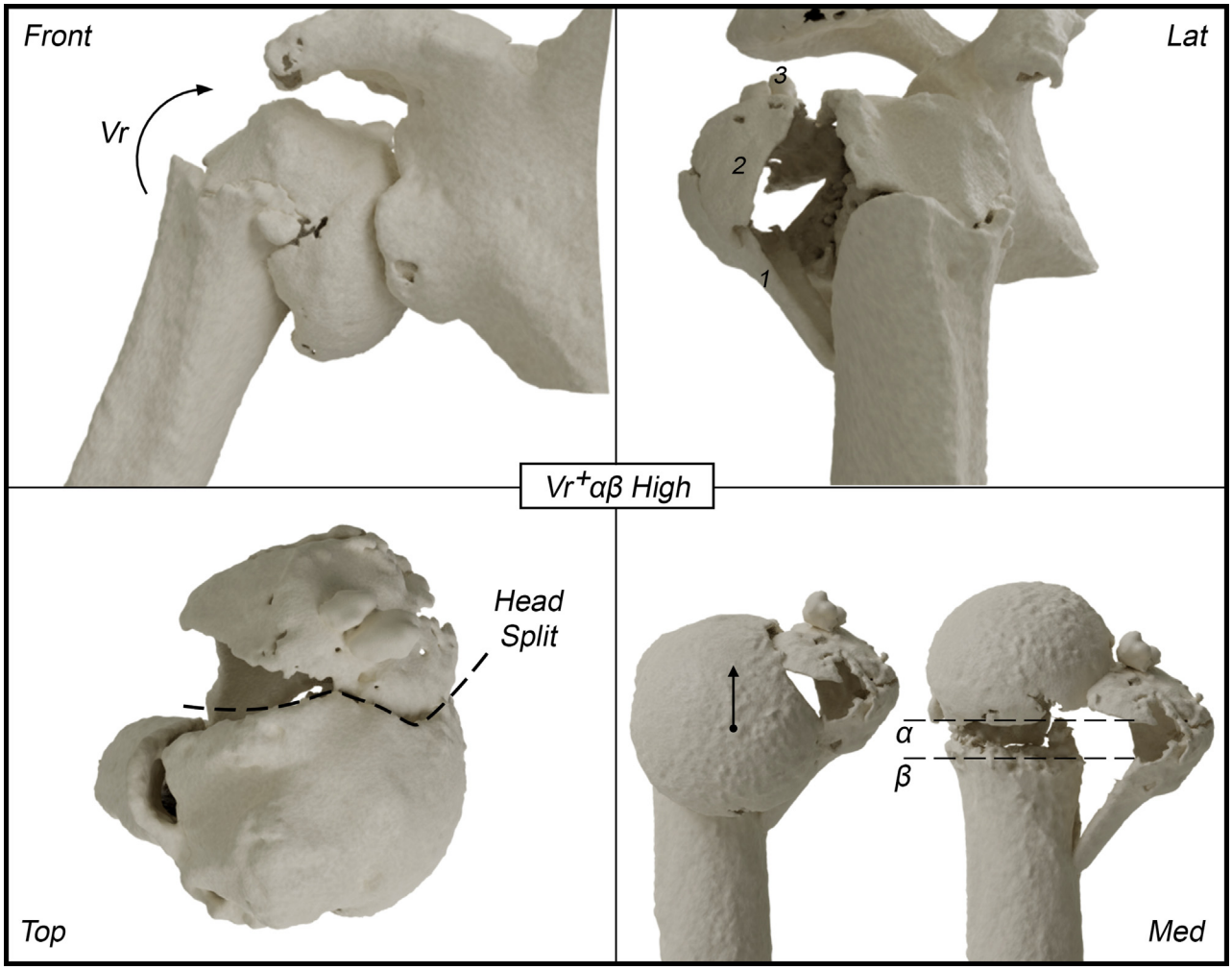

Figure 6 Example of a $Vr^{+}\alpha\beta$ High fracture. 3D reconstruction of one of the 50 fractures analyzed. The 4 quarters show different views: Front (frontal), Lat (lateral), Top, and Med (medial). In the frontal view, the varus displacement of the head is noticeable (Vr). In the top view, the dashed line highlights the head split (+). In the medial view, the arrow indicates the movement needed to the anatomic reposition of the head to better analyze the calcar conditions; the dashed lines show the calcar fracture lines on the α and β planes. In the lateral view, the numbers indicate the fragments of the lateral area (3 fragments of greater tuberosity), and the calcar is unrecognizable (multifragmented under the cephalic cup, level 3 of comminution). The comminution table gives rise to a "high comminution" grade.

principles of the theory to identify fracture patterns precisely, is not so immediate. We believe that a PHF classification could represent an intermediate step that acts as an incipit for the automated system, and at the same time provide a useful tool to equip the surgeon with useful information for fracture analysis.

There is currently no recognized limit threshold above which an interobserver reliability analysis is considered acceptable. Landis and Koch[17] proposed *k* intervals to interpret the strength of the agreement, and these intervals are very often used in studies involving the evaluation of inter- and intraobserver reliability. However, comparison of the *k* values with other studies is not always possible and correct, because this comparison should occur with equal or very similar statistical methods (number of analyzed cases, observers involved, and test methods).

Obviously within the single study, the higher the *k* value, the better the result, but it is referred to personal judgment to hold whether those results are acceptable or not. In our study, the inter- and intraobserver reliability was calculated using Randolph's free-marginal multirater kappa, unlike the canonical Fleiss' *k*,[32] because the raters are not forced to assign a certain number of cases to each category.

The results of the inter- and intraobserver analysis of the proposed classification system, interpreted with the Landis and Koch intervals, showed a moderate to substantial level of agreement with a clear positive trend when using the 3D imaging modality. We consider these results satisfactory and able to attest to the reliability and suitability of the classification.

The new proposed classification, relying on the CV theory, has a solid rational basis for understanding and

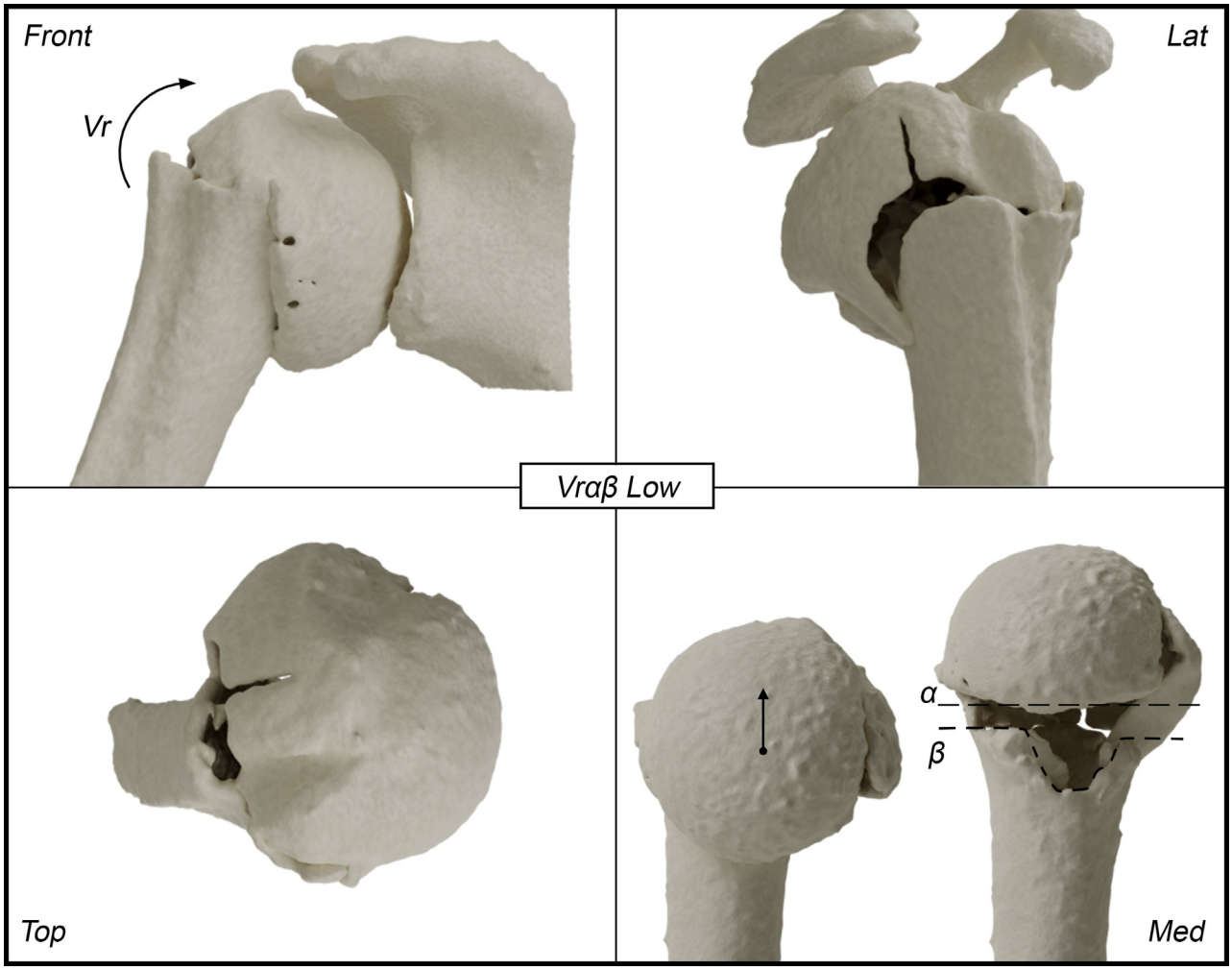

Figure 7 Example of a Vrαβ Low fracture. 3D reconstruction of one of the 50 fractures analyzed. The 4 quarters show different views: Front (frontal), Lat (lateral), Top, and Med (medial). In the frontal view, the varus displacement of the head is noticeable (Vr). In the medial view, the arrow indicates the movement needed to the anatomic reposition of the head to better analyze the calcar conditions; the dashed lines show the calcar fracture lines on the α and β planes. The calcar is unrecognizable (level 3 of comminution), but the lateral area is practically intact (level 0 of lateral comminution), which indicates a ''low comminution'' grade.

justifying the pathologic displacements assumed by the humeral head in impacted fractures. This classification also provides additional information (calcar condition, severity concept, and comminution level) that can be very useful in clinical practice, making further steps toward a correct diagnostic-therapeutic process (Figs. 3-5).

The identification of the α and β planes enables the understanding of the volumetric fracture configuration and defines how the CV, and in particular the calcar, is linked to the head. A fractured calcar completely on the α plane presents a greater risk of necrosis of the humeral head compared with a calcar fractured only on the β plane.

Regarding the tuberosities, we considered the lesser and greater tuberosities within the lateral zone of the CV and not as single parts; this was because we were not interested in the distinction in fracture parts but in a volumetric classification model. Indeed, the CV theory suggests that a humeral head in a valgus position is connected to the involvement of the lateral zone of the CV, and therefore of the tuberosities. Instead, the medial part is generally less involved, also in terms of displacement, and represents a hinge point that is either more or less stable according to the calcar loss. However, the fracture morphology can be very varied and has a decisive weight in the therapeutic choice. We believe that it was appropriate to include an assessment of comminution in the classification system to further differentiate fractures that had the same main fracture pattern but were morphologically very different, and therefore had different possible therapeutic indications. For example, a $Vr^{+}\alpha\beta$ *High* fracture is characterized by involvement of the medial area of the CV, with calcar fractures on both planes, suggesting a loss of the medial support of the epiphysis and a serious risk for humeral head vascularization (aggravated by the presence of the head

split). *Vr*$^{+}$*αβ High* also has an added global condition of high comminution, indicating a difficult recoverability of the original anatomy (Fig. 6). Even if other variables must be considered for the final choice of the most suitable treatment (patient age, comorbidity, functional expectation of the patient, surgeon experience, and soft tissue condition), the information obtained using the proposed classification is very important for the real pathomorphologic understanding of the fracture, as well as for a correct diagnostic-therapeutic procedure.

In another example, a *Vrαβ Low* fracture is also characterized by involvement of the medial zone with calcar fractures on both planes, which suggest a loss of the medial support of the epiphysis and a risk for humeral head vascularization. However, the low degree of global comminution is a positive factor that influences the therapy as operative vs. nonoperative (Fig. 7). Indeed, a volumetric classification that allows the possibility of quantifying the severity according to the calcar comminution, position of the head, or the distal or proximal involvement of the area that controls the vascularization can help the surgeon to consider a more conservative indication than the surgical one, especially in basic emergency hospitals and in elderly patients with fragility fractures.

There are also some limitations to our method of classification. First, this classification only covers impacted fractures, although conceptually it is possible to extend it in the future. Second, the number of studied cases is relatively small, and no comparison has been made with other classifications. Third, the expert surgeon (R.R.) and the evaluators come from a single department, which is likely to have influenced the way in which the fractures were assessed. In the described classification system, the presence of many fracture features can be considered a strength, but these can also affect the interobserver and intraobserver classification reliability. However, the classification reliability has a secondary relevance regarding the purposes of our classification system. Indeed, we propose the use of the classification system as another step for an automation system that will enable immediate identification of the fracture pattern. Future plans will concern the validation of this classification in a clinical setting.

Conclusions

This study outlines a new classification system for proximal humeral impacted fractures based on the CV theory. In this classification, the definition and introduction of a severity concept, accompanied by information on the CV comminution, are the principles used to create a suitable diagnostic-therapeutic process. The results of our reliability analyses were satisfactory, in particular those of the 3D diagnostic imaging, attesting to the reliability and suitability of the classification.

The impacted PFH classification can provide the surgeon with useful information for fracture analysis, and can provide a basis for the generation of an automated system. A synoptic framework can help the surgeon to identify the fracture patterns more easily, and the 3D imaging modality improves the agreement values. This in accordance with Neer's[21] statement that identified the problem of the low reliability, not as a limitation of the classification itself, but rather linked to the poor ability of the surgeon to interpret the images.

Disclaimer

R. Russo, F. Fiorentino, and L. R. Pietroluongo are cofounders in an innovative startup: E-Lisa srl. The company is focused on R&D, consultancy, and formation in the orthopedic and trauma fields. The authors wish to confirm that there are conflicts of interest associated with this publication but there has been no financial support.

References

1. Audigé L, Bhandari M, Hanson B, Kellam J. A concept for the validation of fracture classifications. J Orthop Trauma 2005;19:404-9. https://doi.org/10.1097/01.bot.0000155310.04886.37
2. Audigé L, Bhandari M, Kellam J. How reliable are reliability studies of fracture classifications? A systematic review of their methodologies. Acta Orthop Scand 2004;75:184-94. https://doi.org/10.1080/00016470412331294445
3. Beardsley C, Marsh JL, Brown T. Quantifying comminution as a measurement of severity of articular injury. Clin Orthop Relat Res 2004:74-8. https://doi.org/10.1097/01.blo.0000131637.04391.40
4. Beardsley CL, Bertsch CR, Marsh JL, Brown TD. Interfragmentary surface area as an index of comminution energy: proof of concept in a bone fracture surrogate. J Biomech 2002;35:331-8. https://doi.org/10.1016/S0021-9290(01)00214-7
5. Brooks CH, Revell WJ, Heatley FW. Vascularity of the humeral head after proximal humeral fractures. An anatomical cadaver study. J Bone Joint Surg Br 1993;75:132-6.
6. Chao EYS, Inoue N. Biomechanics of osteoporotic bone and fractures. In: Internal fixation in osteoporotic bone. New York: Thieme; 2002. p. 9-11. https://doi.org/10.1055/b-002-52050
7. Choy G, Khalilzadeh O, Michalski M, Do S, Samir AE, Pianykh OS, et al. Current applications and future impact of machine learning in radiology. Radiology 2018;288:318-28. https://doi.org/10.1148/radiol.2018171820
8. Cole JH, Van Der Meulen MCH. Whole bone mechanics and bone quality. Clinical Orthop Relat Res 2011;469:2139-49. https://doi.org/10.1007/s11999-011-1784-3
9. Erickson BJ, Korfiatis P, Akkus Z, Kline TL. Machine learning for medical imaging. Radiographics 2017;37:505-15. https://doi.org/10.1148/rg.2017160130
10. Foruria AM, de Gracia MM, Larson DR, Munuera L, Sanchez-Sotelo J. The pattern of the fracture and displacement of the fragments predict the outcome in proximal humeral fractures. J Bone Joint Surg Br 2011;93:378-86. https://doi.org/10.1302/0301-620x.93b3.25083

11. Garbuz DS, Masri BA, Esdaile J, Duncan CP. Classification systems in orthopaedics. J Am Acad Orthop Surg 2002;10:290-7. https://doi.org/10.5435/00124635-200207000-00007
12. Gardner MJ, Weil Y, Barker JU, Kelly BT, Helfet DL, Lorich DG. The importance of medial support in locked plating of proximal humerus fractures. J Orthop Trauma 2007;21:185-91. https://doi.org/10.1097/BOT.0b013e3180333094
13. Hernandez D, Garimella R, Eltorai AEM, Daniels AH. Computer-assisted orthopaedic surgery. Orthop Surg 2017;9:152-8. https://doi.org/10.1111/os.12323
14. Hertel R, Hempfing A, Stiehler M, Leunig M. Predictors of humeral head ischemia after intracapsular fracture of the proximal humerus. J Shoulder Elbow Surg 2004;13:427-33. https://doi.org/10.1016/j.jse.2004.01.034
15. Hettrich CM, Boraiah S, Dyke JP, Neviaser A, Helfet DL, Lorich DG. Quantitative assessment of the vascularity of the proximal part of the humerus. J Bone Joint Surg Am 2010;92:943-8. https://doi.org/10.2106/JBJS.H.01144
16. Krappinger D, Bizzotto N, Riedmann S, Kammerlander C, Hengg C, Kralinger FS. Predicting failure after surgical fixation of proximal humerus fractures. Injury 2011;42:1283-8. https://doi.org/10.1016/j.injury.2011.01.017
17. Landis JR, Koch GG. The measurement of observer agreement for categorical data. Biometrics 1977;33:159-74.
18. Lescheid J, Zdero R, Shah S, Kuzyk PRT, Schemitsch EH. The biomechanics of locked plating for repairing proximal humerus fractures with or without medial cortical support. J Trauma 2010;69:1235-42. https://doi.org/10.1097/TA.0b013e3181beed96
19. Li Z, Zhang X, Müller H, Zhang S. Large-scale retrieval for medical image analytics: a comprehensive review. Med Image Anal 2018;43:66-84. https://doi.org/10.1016/j.media.2017.09.007
20. Martin JS, Marsh JL. Current classification of fractures. Rationale and utility. Radiol Clin North Am 1997;35:491-506.
21. Neer CS. Four-segment classification of proximal humeral fractures: purpose and reliable use. J Shoulder Elbow Surg 2002;11:389-400. https://doi.org/10.1067/mse.2002.124346
22. Nichols JA, Herbert Chan HW, Baker MAB. Machine learning: applications of artificial intelligence to imaging and diagnosis. Biophys Rev 2019;11:111-8. https://doi.org/10.1007/s12551-018-0449-9
23. Osterhoff G, Morgan EF, Shefelbine SJ, Karim L, McNamara LM, Augat P. Bone mechanical properties and changes with osteoporosis. Injury 2016;47(Suppl 2):S11-20. https://doi.org/10.1016/S0020-1383(16)47003-8
24. Ponce BA, Thompson KJ, Raghava P, Eberhardt AW, Tate JP, Volgas DA, et al. The role of medial comminution and calcar restoration in varus collapse of proximal humeral fractures treated with locking plates. J Bone Joint Surg Am 2013;95:e113(1-7). https://doi.org/10.2106/JBJS.K.00202
25. Rahman R, Wood ME, Qian L, Price CL, Johnson AA, Osgood GM. Head-mounted display use in surgery: a systematic review. Surg Innov 2020;27:88-100. https://doi.org/10.1177/1553350619871787
26. Randolph JJ. Free-marginal multirater kappa (multirater K[free]): an alternative to Fleiss' fixed-marginal multirater kappa. In: Joensuu learning and instruction symposium. Finland: Joensuu; October 14-15, 2005.
27. Resch H. Proximal humeral fractures: current controversies. J Shoulder Elbow Surg 2011;20:827-32. https://doi.org/10.1016/j.jse.2011.01.009
28. Russo R, Guastafierro A, Pietroluongo LR. A morphovolumetric study of head malposition in proximal humeral fractures based on 3-dimensional computed tomography scans: the control volume theory. J Shoulder Elbow Surg 2018;27:940-9. https://doi.org/10.1016/j.jse.2017.12.004
29. Shehovych A, Salar O, Meyer CER, Ford DJ. Adult distal radius fractures classification systems: essential clinical knowledge or abstract memory testing? Ann R Col Surg Engl 2016;98:525-31. https://doi.org/10.1308/rcsann.2016.0237
30. Solberg BD, Moon CN, Franco DP, Paiement GD. Locked plating of 3- and 4-part proximal humerus fractures in older patients: the effect of initial fracture pattern on outcome. J Orthop Trauma 2009;23:113-9. https://doi.org/10.1097/BOT.0b013e31819344bf
31. Tack P, Victor J, Gemmel P, Annemans L. 3D-printing techniques in a medical setting: a systematic literature review. Biomed Eng Online 2016;15:115. https://doi.org/10.1186/s12938-016-0236-4
32. Warrens MJ. Inequalities between multi-rater kappas. Adv Data Anal Classif 2010;4:271-86. https://doi.org/10.1007/s11634-010-0073-4